Inorganic Chemistry

Article

pubs.acs.org/IC

A Rare Phenoxido/Acetato/Azido Bridged Trinuclear and an Unprecedented Phenoxido/Azido Bridged One-Dimensional Polynuclear Nickel(II) Complexes: Synthesis, Crystal Structure, and Magnetic Properties with Theoretical Investigations on the Exchange Mechanism

Rituparna Biswas,[†] Sandip Mukherjee,[‡] Paramita Kar,[†] and Ashutosh Ghosh*[,†]

[†]Department of Chemistry, University College of Science, University of Calcutta, 92, APC Road, Kolkata-700 009, India

[‡]Department of Inorganic and Physical Chemistry, Indian Institute of Science, Bangalore-560 012, India

Supporting Information

ABSTRACT: The reaction of a tridentate Schiff base ligand HL (2-[(3-dimethylaminopropylimino)-methyl]-phenol) with Ni(II) acetate or perchlorate salts in the presence of azide as coligand has led to two new Ni(II) complexes of formulas $[Ni_3L_2(OAc)_2(\mu_{1,1}\text{-}N_3)_2(H_2O)_2]\cdot 2H_2O$ (**1**) and $[Ni_2L_2(\mu_{1,1}\text{-}N_3)(\mu_{1,3}\text{-}N_3)]_n$(**2**). Single crystal X-ray structures show that complex **1** is a linear trinuclear Ni(II) compound containing a μ_2-phenoxido, an end-on (EO) azido and a *syn-syn* acetato bridge between the terminal and the central Ni(II) ions. Complex **2** can be viewed as a one-dimensional (1D) chain in which the triply bridged (di-μ_2-phenoxido and EO azido) dimeric Ni_2 units are linked to each other in a zigzag pattern by a single end-to-end (EE) azido bridge. Variable-temperature magnetic susceptibility studies indicate the presence of moderate ferromagnetic exchange coupling in complex **1** with J value of 16.51(6) cm^{-1}. The magnetic behavior of **2** can be fitted in an alternating ferro- and antiferromagnetic model [J_{FM} = +34.2(2.8) cm^{-1} and J_{AF} = −21.6(1.1) cm^{-1}] corresponding to the triple bridged dinuclear core and EE azido bridge respectively. Density functional theory (DFT) calculations were performed to corroborate the magnetic results of **1** and **2**. The contributions of the different bridges toward magnetic interactions in both compounds have also been calculated.

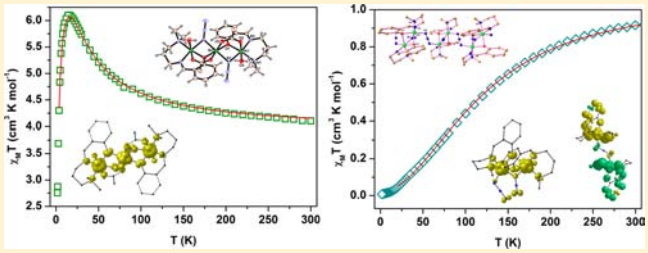

INTRODUCTION

Research on coordination polymers of transition-metals with novel topology has evoked great interest because of their impressive structural diversity and intriguing physical properties.[1,2] Simple paramagnetic metal ions upon linking with appropriate bridging ligands may generate coordination polymers with interesting magnetic properties. Exchange interactions propagated by multiatom bridges between paramagnetic centers that are able to efficiently transmit the magnetic exchange interactions allow the preparation of interesting magnetic materials.[3−5] Among them metal-azido polynuclear complexes deserve special mention because of their fascinating structural diversities, their importance in understanding magneto-structural correlations, and their promising potential applications in functional materials.[6] The main expression of the versatility of this ligand lies in the different coordination modes that it can offer; the most common ones are the end-to-end ($\mu_{1,3}$-N_3, EE) and end-on ($\mu_{1,1}$-N_3, EO) modes. In general, EE azido bridges propagate antiferromagnetic interactions,[7] whereas the EO coordination mode is associated with ferromagnetic coupling;[8] although exceptions to this general statement have been reported.[9] Furthermore, different bridging modes of the azido ions may simultaneously exist in the same species, leading to interesting topologies and magnetic behaviors.[10]

The study of magnetic exchange mediated by azide in its different bridging modes is often complicated by the presence of additional bridging ligands as all these bridges may either add or counterbalance their effects.[11−13] Among the possibilities of innumerable combinations of different bridges, a combination of phenoxido and/or carboxylato groups with the azido ligand in one system is an interesting approach for constructing new materials and for modulating magnetic behaviors as both these ligand can transmit F or AF coupling between metal centers. For the phenoxido bridges, usually when the Ni−O-(phenoxido)−Ni bridging angle is less than 97° ferromagnetic coupling occurs whereas the coupling becomes antiferromagnetic at larger bridging angles.[14] On the other hand, the carboxylate functionality can offer a variety of magnetic interactions depending on its versatile bridging modes *syn−syn*, *anti−anti*, *syn−anti* (Scheme 1). In general, significant

Received: March 14, 2012
Published: July 12, 2012

   dx.doi.org/10.1021/ic300547w | *Inorg. Chem.* 2012, 51, 8150−8160

Scheme 1. Most Common Bridging Modes of Azide (a,b) and (Carboxylate) (c−e) Ligands

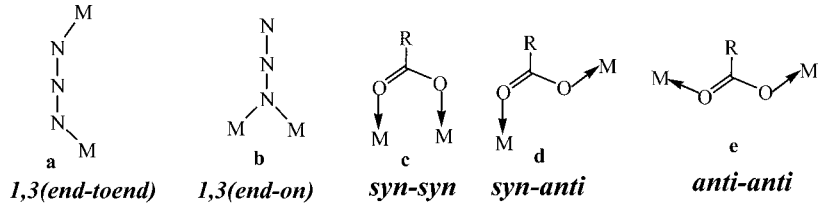

antiferromagnetic interaction between the metal centers is mediated by the *syn−syn* and *anti−anti* carboxylate coordination modes, whereas *syn−anti* mode mediates either weak ferro- or antiferromagnetic interaction.[15] The density functional theory (DFT) study of exchange interactions between paramagnetic metal centers through various bridging ligands has proved to be very fruitful for understanding the fundamental factors governing the magnetic properties of transition-metal compounds.[16]

Herein, we report the crystal structures, magnetic properties, and DFT calculations of a mixed bridged trinuclear Ni(II) compound of formula $[Ni_3L_2(OAc)_2(\mu_{1,1}\text{-}N_3)_2(H_2O)_2]\cdot 2H_2O$ (**1**) and a one-dimensional (1D) polynuclear chain $[Ni_2L_2(\mu_{1,1}\text{-}N_3)(\mu_{1,3}\text{-}N_3)_2]_n$ (**2**). Complex **1** is a rare triple bridged (phenoxido, acetato, and azido) discrete trinuclear Ni(II) compound that shows moderately strong ferromagnetic interaction. Complex **2** is unique in the sense that it is the first polymeric Ni(II) compound in which the dinuclear $[Ni_2(\mu_2\text{-phenoxido})_2(\mu_{1,1}\text{-}N_3)]$ cores are joined by single $\mu_{1,3}\text{-}N_3$ bridges and consequently exhibits alternating ferro- and antiferromagnetic interactions. We also report here DFT calculations to provide a qualitative theoretical interpretation of overall magnetic behavior of the complexes. Such calculations allow us to propose a detailed analysis of the underlying magnetic pathways through the different bridges and also evaluate their individual contributions to the overall exchange interactions.

EXPERIMENTAL SECTION

Materials. The diamine and salicyldehyde were purchased from Lancaster Chemical Co. The chemicals were of reagent grade and used without further purification.

Synthesis of the Schiff-Base Ligand 2-[(3-Dimethylamino-propylimino)-methyl]-phenol (HL). The Schiff base was prepared by the condensation of salicylaldehyde (1.05 mL, 10 mmol) and *N*,*N*-dimethyl-1,3-propanediamine (1.26 mL, 10 mmol) in methanol (10 mL) as reported earlier.[17]

Synthesis of $[Ni_3L_2(OAc)_2(\mu_{1,1}\text{-}N_3)_2(H_2O)_2]\cdot 2H_2O$ (1). $Ni(OAc)_2\cdot 4H_2O$ (1.860 g, 7.5 mmol), dissolved in 10 mL of hot methanol, was added to a methanolic solution (10 mL) of the ligand (HL; 5 mmol) with constant stirring. After about 10 min an aqueous solution (2 mL) of NaN_3(0.438 g, 7.5 mmol) was added with slow stirring followed by addition of triethylamine (0.70 mL, 5 mmol). A light green precipitate appeared immediately. It was then filtered, and the filtrate was left to stand in the air. X-ray-quality single crystals of complex **1** were obtained in 2 days on slow evaporation of the filtrate. Yield: 1.00 g; 70%. *Anal. Calcd.* for $C_{28}H_{48}N_{10}Ni_3O_{10}$: C, 39.07, H, 5.62, N, 16.27. Found: C, 39.11; H, 5.56; N, 16.15. IR (KBr pellet, cm^{-1}): 3461(broad) ν(OH), 1634 ν(C═ N), 1580 ν_{as}(C═O), 1417 ν_s(C═O) and 2086 $\nu_{as}(N_3^-)$. $\lambda_{max}(CH_3OH)$, 368, 634, and 997 nm.

Synthesis of $[Ni_2L_2(\mu_{1,1}\text{-}N_3)(\mu_{1,3}\text{-}N_3)_2]_n$ (2). $Ni(ClO_4)_2\cdot 6H_2O$ (1.828 g, 5 mmol), dissolved in 10 mL of methanol, was added to a methanolic solution (10 mL) of the ligand (HL) (5 mmol) with constant stirring. After about 15 min, an aqueous solution (2 mL) of NaN_3 (0.32 g, 5 mmol) was added to it. A deep green precipitate appeared immediately. It was then filtered and washed with diethyl ether and redissolved in CH_3CN. Needle-shaped deep-green single crystals of **2**, suitable for X-ray diffraction were obtained by layering of the green solution with Et_2O. Yield: 1.02 g; 67%. *Anal. Calcd.* for $C_{12}H_{17}N_5NiO$: C, 47.10, H, 5.60, N, 22.89. Found: C, 47.02; H, 5.65; N, 22.73. IR (KBr pellet, cm^{-1}): 1629 ν(C═ N), 2094 $\nu_{as}(N_3^-)$. $\lambda_{max}(CH_3OH)$, 370, 641, and 995 nm.

Physical Measurements. Elemental analyses (carbon, hydrogen, and nitrogen) were performed using a Perkin-Elmer 240C elemental analyzer. IR spectra in KBr (4500−500 cm^{-1}) were recorded using a Perkin-Elmer RXI FT-IR spectrophotometer. Electronic spectra (1400−350 nm) in CH_3OH (for **1** and **2**) were recorded in a Hitachi U-3501spectrophotometer. The measurements of variable-temperature magnetic susceptibility were carried out on a Quantum Design MPMS-XL7 SQUID magnetometer. Susceptibility data were collected using an external magnetic field of 0.2 T for both the complexes in the temperature range of 1.8 to 300 K. The corrections of measured susceptibilities were carried out considering both the sample holder as the background and the diamagnetism of the constituent atoms according to Pascal's tables.[18]

Crystallographic Data Collection and Refinement. Suitable single crystals of each complexes were mounted on a Bruker SMART diffractometer equipped with a graphite monochromator and Mo−Kα (λ = 0.71073 Å) radiation. The structures were solved using Patterson method by using the SHELXS97. Subsequent difference Fourier synthesis and least-squares refinement revealed the positions of the remaining non hydrogen atoms. Non-hydrogen atoms were refined with independent anisotropic displacement parameters. All the hydrogen atoms bonded to carbon were placed in idealized positions, and their displacement parameters were fixed to be 1.2 times larger than those of the attached non-hydrogen atom and the hydrogen atoms on the water oxygen atoms O(4) and O(4)′ in **1**, which were located in the difference Fourier map. Successful convergence was indicated by the maximum shift/error of 0.001 for the last cycle of the least-squares refinement. Hydrogen atoms at O(5) of water molecule in complex **1** could not be located in the difference Fourier map. All calculations were carried out using SHELXS 97,[19] SHELXL 97,[20] PLATON 99,[21] ORTEP-32,[22] and WinGX systemVer-1.64.[23] Data collection and structure refinement parameters and crystallographic data for the two complexes are given in Table 1.

Computational Methodology. The following computational methodology was used to calculate the exchange coupling constants in the reported complexes.[24−27] The phenomenological Heisenberg Hamiltonian $H = -\Sigma_{(i>j)}J_{ij}S_iS_j$ (where S_i and S_j are the spin operators of the paramagnetic metal centers i and j, and the J_{ij} parameters are the exchange-coupling constants for the different pairwise interactions between the paramagnetic metal centers of the molecule) can be used to describe the exchange coupling between each pair of transition-metal ions present in the polynuclear complex to construct the full Hamiltonian matrix for the entire system.

To calculate the exchange coupling constants for any polynuclear complex with n different exchange constants, at least the energy of n + 1 spin configurations must be calculated. For example, in the case of the studied dinuclear model complexes, the exchange coupling value J were obtained by taking into account the energy of three different spin distributions: quintet with S = 2, triplet with S = 1, and singlet with S = 0, taking the average of the two energy differences obtained from the three spin states.[28]

The hybrid B3LYP functional[29] has been used in all calculations as implemented in the Gaussian 03 package,[30−33] Triple-ζ quality basis

dx.doi.org/10.1021/ic300547w | Inorg. Chem. 2012, 51, 8150−8160

Table 1. Crystallographic Data for Complexes 1 and 2

	1	2
formula	$C_{28}H_{44}N_{10}Ni_3O_8{\cdot}2(H_2O)$	$C_{12}H_{17}N_5NiO$
M	860.82	306.00
crystal system	monoclinic	orthorhombic
space group	$P21/n$ (No. 14)	$Pbcn$ (No. 60)
a/Å	12.491(5)	17.8499(18)
b/Å	10.176(5)	13.2590(13)
c/Å	14.888(5)	11.9339(12)
α/deg	90	90
β/deg	92.439(5)	90
γ/deg	90	90
V/Å^3	1890.7(14)	2824.4(5)
Z	2	8
D_c/g cm^{-3}	1.505	1.439
μ/mm^{-1}	1.542	1.373
F (000)	892	1280
R(int)	0.084	0.074
total reflections	24558	33083
unique reflections	5112	3106
$I > 2\sigma(I)$	3219	2214
R1, wR2	0.0553, 0.1710	0.0370, 0.0980
temp (K)	293	293

Scheme 2. Formation of the Complexes 1 and 2

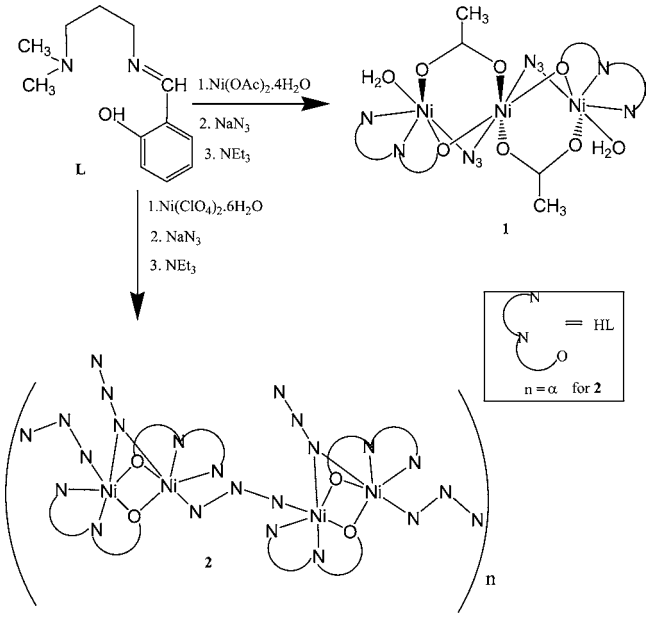

set (TZVP) proposed by Ahlrichs and co-workers have been used for Ni atoms, while 6-31 g(d) basis set was used for other atoms.[34] A quadratic convergence method was employed in the self-consistent field (SCF) process.[35]The calculations were performed on the complexes built from the experimental geometries.

RESULTS AND DISCUSSION

Synthesis of the Complexes. For complex **1**, the tridentate N,N,O donor Schiff base ligand HL (2-[(3-dimethylamino-propylimino)-methyl]-phenol) is allowed to react with nickel(II) acetate in methanolic solution, followed by addition of aqueous solution of NaN_3 in a 2:3:2 molar ratio. The triethylamine was added to deprotonate the Schiff base. Under this conditions, the mixed bridged trinuclear complex is produced by the self-assembly of two mono(Schiff base) Ni(II) complexes, one Ni(II), two azide, and two acetate ions (Scheme 2). A very similar procedure is followed for the synthesis of complex **2** except that a methanolic solution of nickel(II) perchlorate is used in place of nickel(II) acetate. However, the composition and structure of complex **2** is very different from that of **1**. It is a polynuclear 1D chain in which the double phenoxido and $\mu_{1,1}$-azido bridged dinuclear units are linked by $\mu_{1,3}$-azido bridges.

IR and UV−vis Spectra of Complexes. In the IR spectra of complexes **1** and **2** a strong and sharp band due to azomethine υ(C═N) appears at 1634 and 1629 cm^{-1} respectively. Complex **1** exhibits one distinct band at 2086 cm^{-1}, consistent with the presence of only one type of azido bridge in the structure. The appearance of a broad band near 3461 cm^{-1} indicates the presence of water molecules in the complex. The IR spectral bands in the 1300−1650 cm^{-1} region are difficult to be attributed because of the appearance of several absorption bands from both the Schiff base and the carboxylate ligands. Nevertheless, by comparing the IR spectra of other Ni(II) complexes of the same ligand,[17] the strong bands at 1580 cm^{-1} may be assigned to the antisymmetric stretching mode of the carboxylate group, whereas the bands at 1417 cm^{-1} to the symmetric stretching modes of the carboxylate ligands in complex **1**. For the polynuclear complex **2**, a sharp band at 2094 cm^{-1} with a hump at 2055 cm^{-1} indicates the presence of two different types of azido groups.

The electronic spectra of these compounds are recorded in methanol solution. The electronic spectra show absorption bands at 634 and 997 nm (for **1**), 641 and 995 nm (for **2**). These bands are assigned to the spin allowed transitions $^3A_{2g}\rightarrow{}^3T_{1g}$, $^3A_{2g}\rightarrow{}^3T_{2g}$(P), respectively. The higher energy d−d bands are obscured by strong ligand to metal charge-transfer transitions. The bands observed at 368, 370 nm for complexes **1** and **2**, respectively, are assigned to those of L→M charge transfer transitions which are characteristic of the transition metal complexes with Schiff base ligands.[36]

Description of the Crystal Structures. *Compound $[Ni_3L_2(OAc)_2(\mu_{1,1}\text{-}N_3)_2(H_2O)_2]{\cdot}2H_2O$ (1).* The crystal structure of **1** consists of discrete centro-symmetric trinuclear unit of formula $[Ni_3L_2(OAc)_2(\mu_{1,1}\text{-}N_3)_2(H_2O)_2]$ together with two solvent water molecules. The structure is shown in Figure 1 together with the atomic numbering scheme. Selected bond distances and angles are listed in Table 2. In the structure, the three Ni(II) centers are interlinked through three different

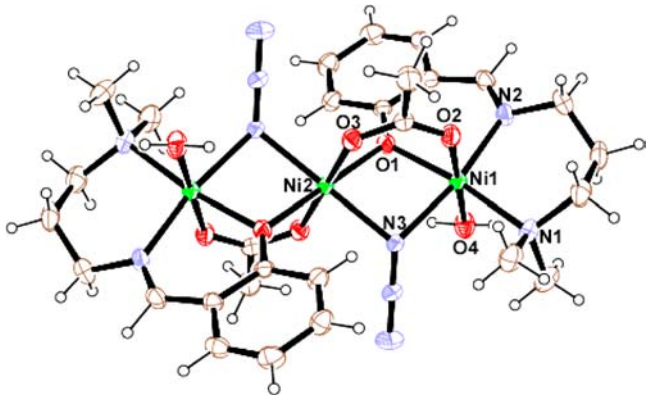

Figure 1. ORTEP view of complex **1** with ellipsoids at the 30% probability level.

dx.doi.org/10.1021/ic300547w | Inorg. Chem. 2012, 51, 8150−8160

Table 2. Bond Distances (Å) and Angles (deg) in the Metal Coordination Spheres of Complex 1[a]

atoms	distance	atoms	angle
Ni(1)—O(1)	2.023(3)	O(1)–Ni(1)—O(2)	90.66(11)
Ni(1)—O(2)	2.057(3)	O(1)–Ni(1)—O(4)	88.89(14)
Ni(1)—O(4)	2.114(4)	O(1)–Ni(1)—N(1)	171.69(14)
Ni(1)—N(1)	2.177(3)	O(1)–Ni(1)—N(2)	89.95(15)
Ni(1)—N(2)	2.040(4)	O(1)–Ni(1)—N(3)	78.97(12)
Ni(1)—N(3)	2.112(3)	O(2)–Ni(1)—O(4)	179.54(15)
Ni(2)—O(1)	2.051(3)	O(2)–Ni(1)—N(1)	88.31(13)
Ni(2)—O(3)	2.071(3)	O(2)–Ni(1)—N(2)	88.68(14)
Ni(2)—N(3)	2.089(3)	O(2)–Ni(1)—N(3)	92.54(13)
		O(4)–Ni(1)—N(1)	92.15(16)
		O(4)–Ni(1)—N(2)	91.26(15)
		O(4)–Ni(1)—N(3)	87.44(15)
		N(1)–Ni(1)—N(2)	98.27(16)
		N(1)–Ni(1)—N(3)	92.83(13)
		N(2)–Ni(1)—N(3)	168.87(15)
		O(1)–Ni(2)—O(3)	89.08(11)
		O(1)–Ni(2)—N(3)	78.88(12)
		O(3)–Ni(2)—N(3)	90.98(13)
		Ni(1)–O(1)—Ni(2)	99.50(13)
		Ni(2)–N(3)—N(4)	122.9(3)
		Ni(1)–N(3)—Ni(2)	95.51(12)
		Ni(1)–N(3)—N(4)	128.6(3)

[a] ′ = 2 − *x*, −*y*, 2 − *z*.

kinds of bridges (EO-azido, μ_2-phenoxido, and *syn-syn* acetato). The central Ni^{2+} ion lies on an inversion center. The structure may be assumed to be composed of two terminal mononuclear units of $[NiL(N_3)H_2O]$ connected by a central $[Ni(OAc)_2]$ unit through the nitrogen atoms of EO-azide, phenoxido oxygen atoms of the Schiff base ligand, and the oxygen atoms of *syn-syn* acetate anions. There are two crystallographically independent Ni(II) ions in the molecule with different coordination environments. Each of the two equivalent terminal Ni(1) atoms reside in a $[N_3O_3]$ octahedral environment where three donor atoms of the tridentate Schiff base ligand, with dimensions Ni(1)–N(1) 2.177(3) Å, Ni(1)–N(2) 2.040(4) Å, and Ni(1)–O(1) 2.023(3) Å, together with the azide nitrogen atom N(3) at 2.112(3) Å constitute the equatorial plane. Two axial positions are occupied by one oxygen atom of the bidentate acetate ion O(2) [Ni(1)–O(2) = 2.057(3) Å] and another oxygen atom O(4) of water molecule [Ni(1)–O(4) = 2.114(4) Å]. The deviations of the coordinating atoms N(1), N(2), N(3), and O(1) from the mean plane passing through them are 0.018(4) Å, −0.020(4) Å, −0.022(4) Å, and 0.023(3) Å, respectively, and that of Ni(1) from the same plane is −0.003(5) Å. The central Ni(2) is also hexacoordinated with a centrosymmetric $[N_2O_4]$ *trans*-octahedral environment furnished by two oxygen atoms of bridging acetate groups (O(3) and O(3)′) (′ = 2 − *x*, −*y*, 2 − *z*) and two μ_2-phenoxido oxygen atoms (O(1) and O(1)′) in the basal plane [Ni(2)–O(3) = 2.071(3) Å and Ni(2)–O(1) = 2.051(3) Å] and two μ-1,3-azide nitrogen atoms (N(3) and N(3)′) in the two axial positions [Ni(2)–N(3) = 2.089(3) Å]. Adjacent Ni(II) atoms are separated by 3.110(2) Å. Two bridging Ni(1)–N(3)–Ni(2) and Ni(1)–O(1)–Ni(2) angles are 95.51(12)° and 99.50(13)°, respectively.

Compound $[Ni_2L_2(\mu_{1,1}\text{-}N_3)(\mu_{1,3}\text{-}N_3)]_n$ (**2**). The structure of complex **2** contains neutral dimeric units formulated as $[Ni_2L_2(N_3)_2]$ (Figure 2), which are further joined together by single $\mu_{1,3}$-azido bridges to form a 1D chain. A crystallographic 2 fold rotational axis of symmetry passes through the three nitrogen atoms of the bridging EO azide. Selected bond lengths and angles are summarized in Table 3. The dimeric unit, $[Ni_2L_2(N_3)_2]$ consists of two equivalent nickel atoms, Ni(1) and Ni(1)′, (′ = −*x*, *y*, 1/2 − *z*) presenting an elongated octahedral environment formed by the coordination of the deprotonated tridentate Schiff base ligand (L) through the secondary amine nitrogen atom N(1), imine nitrogen atom N(2), and phenoxido oxygen atoms O(1) and O(1)′, and two azide nitrogen atoms N(3) and N(5) with bond distances in the expected range (Table 3). In the dinuclear units two Ni(II) centers are triply bridged through one EO azide nitrogen atom N(5) and two μ_2-phenoxido oxygen atoms O(1) and O(1)′, leading to a short Ni···Ni distance of 2.857 Å. The two phenoxido bridging angles are Ni(1)–O(1)–Ni(1)′ = 85.86(6)° and the azide bridging angle is Ni(1)–N(5)–Ni(1)′ = 86.12(10)°. Each bridging phenoxido oxygen atom is asymmetrically bound, with one Ni–O bond slightly shorter [Ni(1)–O(1) = 2.008(2) Å] than the other [Ni(1)–O(1)′ = 2.182(2) Å]. Whereas the bridging $\mu_{1,1}$-azide is bonded symmetrically with Ni(1)–N(5) bond distances at 2.092(2) Å. These distances are within the range (2.09–2.25 Å) of the reported azido-bridged dinuclear Ni(II) complexes.[6c–e] Ni(1) atom is also bonded to the $\mu_{1,3}$-azide through the nitrogen atom

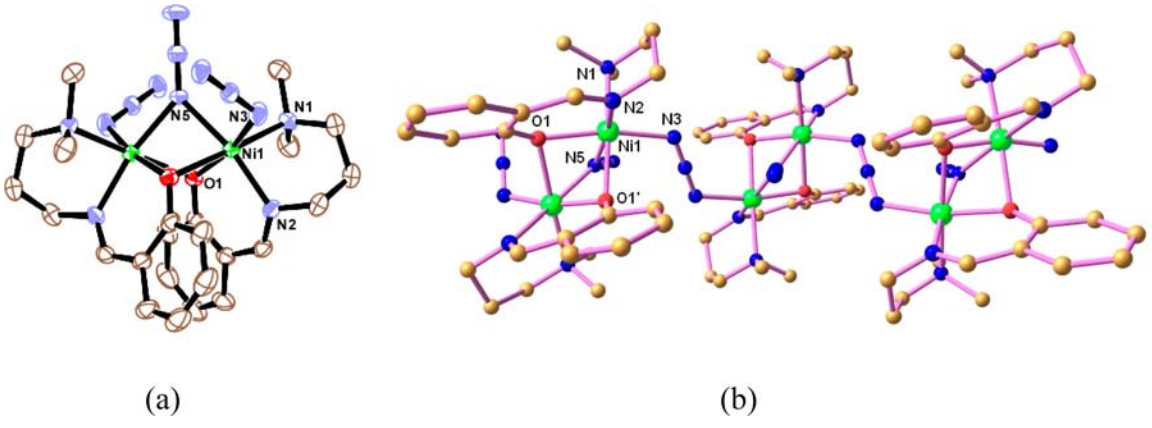

Figure 2. (a) ORTEP-3 view of complex **2** with ellipsoids at the 30% probability level, Hydrogen atoms are omitted for clarity. (b) Ball and stick representation of 1D polymeric structure of complex **2**.

dx.doi.org/10.1021/ic300547w | *Inorg. Chem.* 2012, 51, 8150–8160

Table 3. Bond Distances (Å) and Angles (deg) in the Metal Coordination Spheres of Complex 2[a]

atoms	distance	atoms	angle
Ni(1)—O(1)	2.008(2)	O(1)–Ni(1)—N(1)	98.47(8)
Ni(1)—N(1)	2.151(2)	O(1)–Ni(1)—N(2)	90.88(8)
Ni(1)—N(2)	2.010(2)	O(1)–Ni(1)—N(3)	168.10(8)
Ni(1)—N(3)	2.066(2)	O(1)–Ni(1)—N(5)	79.98(6)
Ni(1)—N(5)	2.092(2)	O(1)–Ni(1)—O(1)′	79.88(7)
Ni(1)—O(1)′	2.182(2)	N(1)–Ni(1)—N(2)	85.58(9)
		N(1)–Ni(1)—N(3)	90.54(9)
		N(1)–Ni(1)—N(5)	101.89(7)
		O(1)′–Ni(1)—N(1)	177.57(8)
		N(2)–Ni(1)—N(3)	97.60(10)
		N(2)–Ni(1)—N(5)	168.89(8)
		O(1)′–Ni(1)—N(2)	96.20(8)
		N(3)–Ni(1)—N(5)	90.60(8)
		O(1)′–Ni(1)—N(3)	90.87(8)
		O(1)′–Ni(1)—N(5)	76.11(6)
		Ni(1)–O(1)—Ni(1)′	85.86(6)
		Ni(1)–N(3)—N(4)	118.60(16)
		Ni(1)–N(5)—N(6)	136.94(5)
		Ni(1)–N(5)—Ni(1)′	86.12(10)

[a] ′ = −x, y, 1/2 − z.

N(3) at 2.066(2) Å and Ni(1)–N(3)–N(4) angle is 118.60(16)°. The sets of four donor atoms O(1), N(2), N(3), N(5) describe the basal plane of Ni(1) and the deviations of these coordinating atoms from the least-squares mean plane through them are −0.008(2), 0.007(2), −0.007(2), and 0.008(2) Å, respectively. The Ni(1) atom is displaced 0.131(1) Å from the same plane toward the axially coordinated N(1) atom. The basal bond lengths around the Ni(1) atom are in the range of 2.008(17)–2.092(2) Å. The axial bond lengths are Ni(1)–O(1)′ 2.182(2) Å and Ni(1)–N(1) 2.151(2) Å.

Magnetic Properties. Figure 3a shows the temperature dependence of χ_M and $\chi_M T$ values for complex **1**. As can be seen, complex **1** shows room temperature $\chi_M T$ value of about 4.10 cm^3 K mol^{-1} per Ni_3 unit. When the temperature is lowered, $\chi_M T$ increases gradually to reach a maximum value of 6.10 cm^3 K mol^{-1} at 15 K followed by a pronounced drop to a value of about 2.75 cm^3 K mol^{-1} at 1.8 K. This increase in $\chi_M T$ value with lowering temperature represents a characteristic feature of intramolecular ferromagnetic interactions between the nickel ions. The sharp decrease of $\chi_M T$ value at very low temperature region may be attributed either to zero-field splitting factor in the $S = 3$ ground spin state or to a contribution arising from intertrimer antiferromagnetic interactions. Thus, we have tried to fit the magnetic properties of this compound to a simple $S = 1$ linear trimer model with the Hamiltonian $H = -J(S_1S_2+S_2S_3) - J'S_1S_3$ where the exchange coupling constant between the terminal ions is considered as negligible ($J' = 0$) and J represents the exchange coupling constant between neighboring nickel centers. The M (in $N\beta$ units) against H/T (in tesla/K units) plots at three different temperatures (Figure 3b, inset) under different applied fields clearly showed the absence (the curves superimpose on each other) of any significant anisotropy in the system. Therefore, we have considered molecular field approximation to include the intertrimer interaction (zJ') term. So, taking the above isotropic spin Hamiltonian and molecular field approximation, we have fitted the magnetic susceptibility data with eq 1.

$$\chi_M = \chi'_M/\{1 - \chi'_M(2zJ'/Ng^2\beta^2)\} \quad (1)$$

$$\chi'_M = (Ng^2\beta^2/3kT)[A/B]$$

where $A = [36 + 6\exp(J/kT) + 30\exp(2J/kT) + 6\exp(-2J/kT) + 84\exp(3J/kT)]$ and $B = [8 + 3\exp(J/kT) + \exp(-J/kT) + 5\exp(2J/kT) + 3\exp(-2J/kT) + 7\exp(3J/kT)]$.

The above model provides a good fit over the temperature range 3.5–300 K. Best fitting results lead to the following parameters: $g = 2.272(8)$, $J = 16.51(6)$ cm^{-1}, $zJ' = -0.24(1)$ cm^{-1} and $R = 1.2 \times 10^{-5}$ {R is the agreement factor defined as $R = \sum[(\chi_M)_{exp.} - (\chi_M)_{calcd.}]^2/\sum(\chi_M)_{exp.}^2$}.

The ferromagnetic coupling in compound **1** leading to $S = 3$ ground spin state is also confirmed by the isothermal magnetization measurement at 2 K (Figure 3b). The saturation is almost reached above 5 T, and the magnetization value at this field is as expected a little higher than $6N\beta$ for an $S = 3$ spin state with g just above 2 (with $g = 2$ the expected value is exactly $6N\beta$).

The χ_M vs T and the $\chi_M T$ vs T plots for compound **2** are shown in Figure 4. The molar susceptibility increases when the temperature decreases. At room temperature the χ_M value is close to 3.04×10^{-3} cm^3 mol^{-1} and it reaches a maximum (4.51×10^{-3} cm^3 mol^{-1} at 110 K for (**2**)), and below these temperatures the curve decreases continuously to 10 K. The

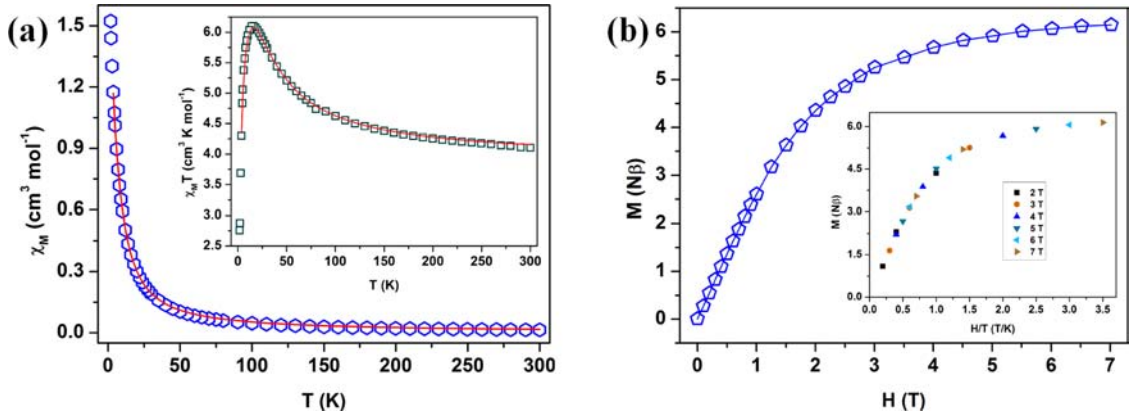

Figure 3. (a) Plots of χ_M vs T and $\chi_M T$ vs T (inset) for complex **1** in the temperature range of 1.8–300 K. The red solid lines indicate the fitting using the theoretical model (see text). (b) Isothermal magnetization for compound **1** at 2 K (the solid line is only guide for the eye) and plots of M vs H/T for temperatures 2, 5, and 10 K at the indicated fields (inset).

dx.doi.org/10.1021/ic300547w | Inorg. Chem. 2012, 51, 8150–8160

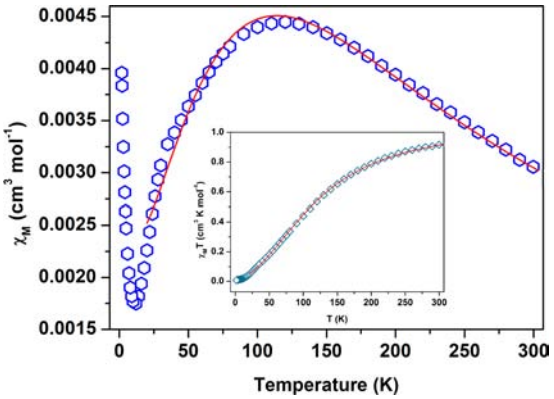

Figure 4. Plots of χ_M vs T and $\chi_M T$ vs T (inset) for complex **2** in the temperature range of 1.8−300 K. The red solid lines indicate the fitting using theoretical model (see text).

next increase in the χ_M values is indicative of the presence of a small quantity of paramagnetic impurities. $\chi_M T$ decreases continuously from room temperature and tends to zero at 4 K (inset $\chi_M T$ vs T plot). According to the structural data, a ferromagnetic interaction between the Ni(II) is expected via both μ_2-phenoxido and EO azide whereas an antiferromagnetic interaction should occur through EE azide bridges. Thus it can be considered as a 1D system with $S = 1$ exhibiting alternating ferro- and antiferromagnetic interactions. The Hamiltonian for the Heisenberg alternating ferro and antiferromagnetic chain can be written as in eq 2 where N is the number of spin pairs, J_{AF} and J_{FM} are the nearest neighbor antiferro- and ferromagnetic exchange interactions.

$$H = -\sum_{i=1}^{N-1}\left(J_{AF}S_{2i}S_{2i+1} + J_{FM}S_{2i}S_{2i-1}\right) \quad (2)$$

We used the method developed by Escuer et al.[37] for this kind of alternating systems to fit magnetic data, defining $\alpha = J_{FM}/|J_{AF}|$.

A good fit is possible only down to 20 K because neither zero-field splitting nor the Haldane gap effect[38] is taken into account. The fit of the experimental data with the above equation (20−300 K) gave the best parameters $J_{AF} = -21.6(1.1)$ cm^{-1}, $\alpha = 1.58(5)$ [$0 \le \alpha \le 2$], $g = 2.034(9)$ and $R = 7.8 \times 10^{-9}$. This implies that $J_{FM} = \alpha|J_{AF}| = +34.2(2.8)$ cm^{-1}.

DFT Calculations. To obtain a better understanding of the magnetic exchange mechanism through the three different bridging pathways in complexes **1** and **2**, quantum mechanical DFT calculations were performed using the GAUSSIAN 03 package with broken symmetry formalism. The theoretical calculation consistently predicted the ferromagnetic ground state for **1** as was found experimentally. However, the theoretical magnetic coupling constants obtained from broken-symmetry calculation for complex **1** is $J = +32$ cm^{-1} which is rather high compared to the experimental result ($J = +16.1(1)$ cm^{-1}). Both experimental and theoretical exchange coupling values are quite low as the antiferromagnetic coupling via acetate bridges decreases the positive exchanges exerted from the small angles of phenoxido and EO azido bridges. It is well established in the literature that the exchange parameters are roughly additive in nature. So the next set of calculations was carried out for a model species **1b**, obtained by eliminating the acetate bridges from the triple bridged compound. The J value as expected is increased (+43 cm^{-1}) for model **1b** (lacking the acetates) (Figure 5), but only slightly. This implies that although the acetates exchange antiferromagnetically, the magnitude is not very high (which is supported by the low spin densities on the bridging atoms of the acetate ligands in all the spin states (Figure 6)).

To obtain a rough idea about the exchange strengths of the azido and the phenoxido groups another set of calculations were performed by eliminating the azido groups (model **1c**). J value decreases to a value of +18 cm^{-1} as expected. From **1a** to **1c** there is roughly ((32−18)/32)×100 = 44% decrease in the J value, which suggests that the azido group is a weaker positive coupler as compared to the phenoxido group for this system.

Spin distribution analysis throws light on the nature and extent of magnetic interaction that takes place between the paramagnetic centers. Several mechanisms are known that can explain qualitatively the coupling interactions between the paramagnetic centers. Among them the spin delocalization mechanism successfully explains the coupling mechanism. It describes the delocalization of spin of the paramagnetic centers over the whole system. However, in most of the transition-metal complexes the spin density concentrates mostly on the metal centers. Mulliken spin density distribution analysis of each spin state of both the model **1b** and **1c** complexes also reveals that acetate bridges transmits weak antiferromagnetic interaction which is supported by the low spin densities on the bridging atoms of the acetate ligands in all the spin states. But the azide ligands show strong ferromagnetic interaction due to

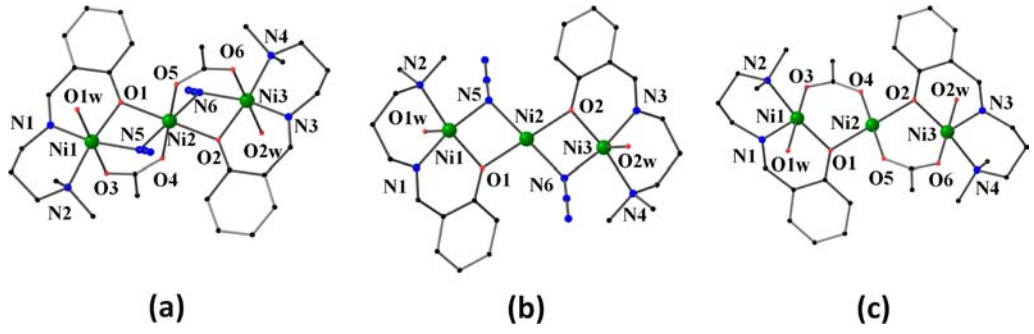

Figure 5. Systems used for computational studies of complex **1**. (a) Trinuclear ferromagnetic unit with two phenoxido, two EO azido and two acetato bridges, $[Ni_3(L)_2(OAc)_2(N_3)_2(H_2O)_2]$; (b) trinuclear ferromagnetic unit with two phenoxido and EO azido bridges, $[Ni_3(L)_2(N_3)_2(H_2O)_2]^{2+}$; (c) trinuclear antiferromagnetic unit with two phenoxido and acetato bridges, $[Ni_3(L)_2(OAc)_2(H_2O)_2]^{2+}$. H atoms have been removed for clarity.

dx.doi.org/10.1021/ic300547w | Inorg. Chem. 2012, 51, 8150−8160

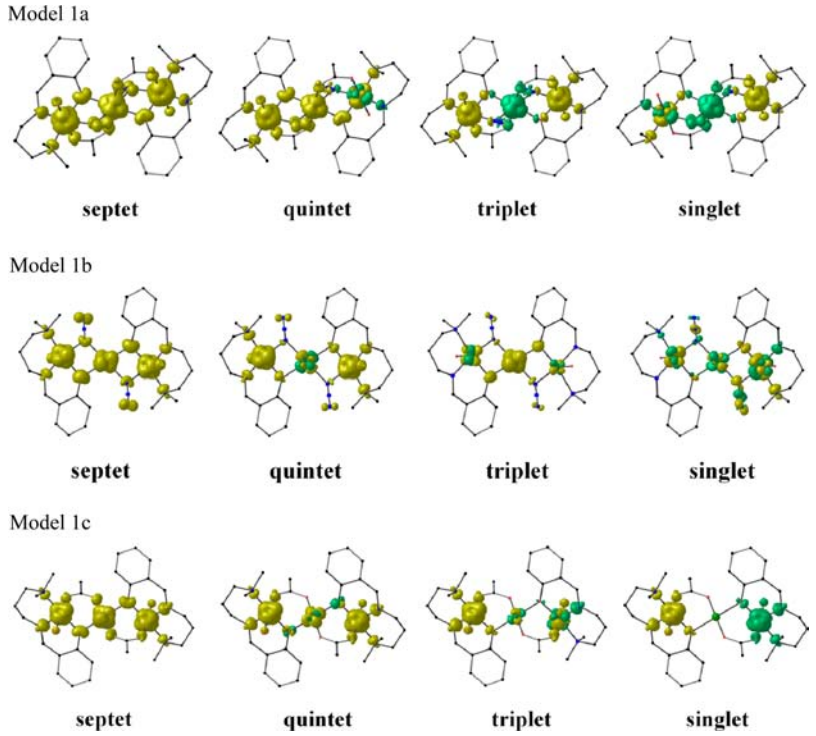

Figure 6. Spin density maps for all the three model complexes **1a**, **1b**, and **1c**, calculated in the B3LYP level for the single determinant corresponding to their each state. α and β spins are represented by yellow and green surfaces. The isodensity surfaces correspond to a value of 0.0025 e/b^3.

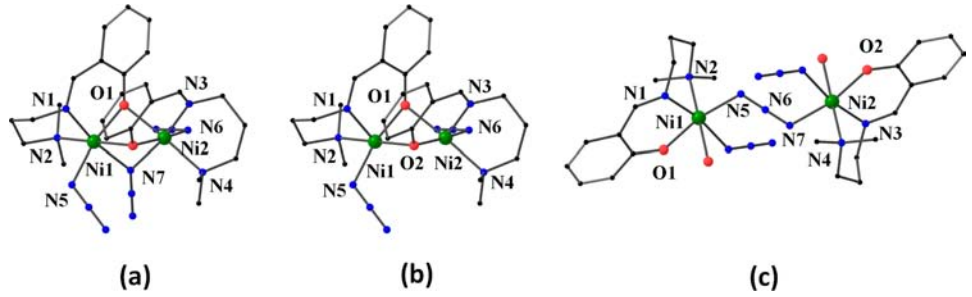

Figure 7. Systems used for computational studies for **2**. (a) Dinuclear ferromagnetic unit with two phenoxido and one EO azido bridge, (b) dinuclear ferromagnetic unit with two phenoxido bridges, (c) dinuclear antiferromagnetic unit with single end-to-end azido bridge.

the considerable spin density distribution over the bridging N atoms of the azide groups. Molecular orbital analysis also supports overall ferromagnetic interaction between the Ni(II) ions in complex **1**. The magnetic orbitals are composed of Ni(II) $d_{x^2-y^2}$ and d_{z^2} orbitals and ligands' orbitals. The considerable contribution of the ligands' orbitals to the magnetic orbitals is responsible for the moderate strong ferromagnetic interaction in **1**. The spin-density distribution plots for the three models in all their spin-states are shown in Figure 6 and the corresponding Mulliken Spin-Density values are given in the Supporting Information, Table S1. The first thing to notice in all these plots is that the metal atoms have decreased spin populations and the bridging atoms have considerable amounts of spin-populations on them (spin-delocalization), which illustrates the spin exchange pathways. For example, for model **1a** in the ground septet spin state the Ni atoms have Mulliken spin densities of about 1.65 au each (while isolated Ni atoms are expected to have 2.00 au, for two unpaired electrons); while the phenoxido O atoms (O(1) and O(2), Figure 5a) have about 0.10 au, the azido bridging N atoms (N(5) and N(6)) have about 0.06 au and the acetate bridging O atoms (O(3), O(4), O(5), and O(6)) have about 0.05 au of Mulliken spin-densities (as the state represents the high-spin state all these values are positive). Also, from the spin density plots it can be easily seen that the lobes of the orbitals on the metal atoms containing the unpaired electrons are directed along the bonding axes, which indicates that the magnetic orbitals on the metal atoms must be of e_g symmetry (this is normally expected for octahedral geometry for a d^8 system, as the $d_{x^2-y^2}$ and d_{z^2} orbitals contain the unpaired electrons).

For **2**, our main aim is to investigate the origin of ferro and antiferro magnetic coupling interaction between the two paramagnetic Ni(II) centers through the bridging phenoxido and azido (both EO and EE) ligands. Thus, for simplicity we reduced the polymeric structure of **2** to model dimeric fragments, $[Ni_2(L)_2(N_3)_3]^-$ (**2a**), $[Ni_2(L)_2(N_3)_2]$ (**2b**), and $[Ni_2(L)_2(N_3)_3(O)_2]^{5-}$ (**2c**), respectively (Figure 7). In calculation, the geometric configurations of the model complexes are taken from the experimental crystal structure data.

dx.doi.org/10.1021/ic300547w | Inorg. Chem. 2012, 51, 8150−8160

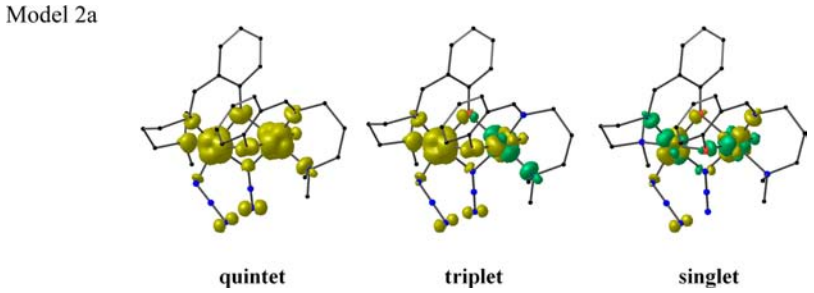

Figure 8. Spin density maps calculated for the spin states of the model complex **2a** at B3LYP level. Positive and negative spin populations are represented as yellow and green surfaces. The isodensity surfaces correspond to a value of 0.0025 e/b^3.

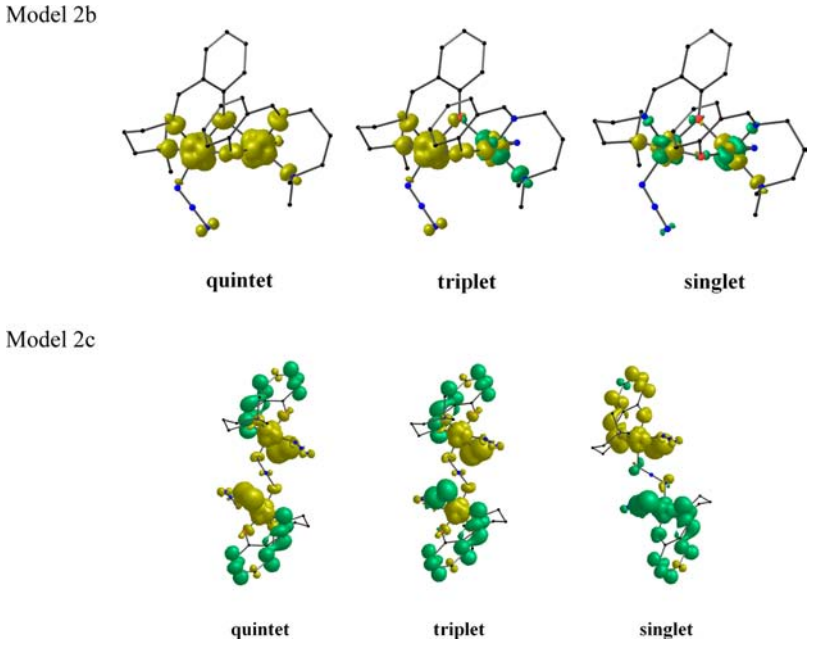

Figure 9. Spin-density maps calculated for **2b** and **2c** at the B3LYP level for all spin states. Positive and negative spin populations are represented as yellow and green surfaces. The isodensity surfaces correspond to a value of 0.0025 e/b^3.

In this case the molecular structure of the complex **2** suggests that the exchange parameter J so obtained, arises primarily because of three superexchange pathways. The calculated exchange coupling constants J_1 = +59 cm^{-1} (from **2a**) and J_2 = −32 cm^{-1} (from **2c**) though high, are consistent with the experimental results of J_{FM} = +34.2(2.8) cm^{-1} and J_{AF} = −21.6(1.1) cm^{-1}. Note that although the calculated values are higher in magnitude, the prediction for the value of α = 59/32 = 1.84, which is more important for the alternating chain system, is quite satisfactory when compared to the experimental result (α = 1.58). We have also performed some DFT calculations to get better qualitatively insight into the role of each bridging group toward the exchange coupling constant of the molecule. When the EO azido group was removed from the ferromagnetic dimer unit (**2b**) the J value reduced to +42 cm^{-1}, indicating that this azido group is responsible for roughly 29% of the overall ferromagnetic exchange, and the rest is equally shared by the two equivalent phenoxido bridges.

The spin-density distribution plots for the three models of **2** in all their spin-states are shown in Figures 8 and 9, and the corresponding Mulliken Spin-Density values are given in the Supporting Information, Table S2.

Although the theoretical and experimental results agree in sign, the magnitude of J values obtained by DFT calculations are considerably higher than the experimental ones. This may be attributed to either the intrinsic limitations of the method, the flexibility of the structures that allow structural changes when the sample is cooled, or simply the fact that the basic units are not magnetically isolated, as indicated by the intercluster exchange parameter.

Magnetostructural Correlations. To understand the ferromagnetic coupling exhibited by complex **1**, one has to focus on the simultaneous presence of three exchange pathways through μ_2-phenoxido, *syn-syn* carboxylate, and the EO azido bridges (Figure 10). Among them, it is well-known that the *syn-syn* conformation of carboxylate ligands cause antiferromagnetic coupling, EO azido bridges transmit ferromagnetic coupling whereas μ_2-phenoxido bridges can transmit either antiferro or ferromagnetic interaction depending upon Ni−O(phenoxido)−Ni bridging angles.[39] To the best of our knowledge, among the structurally and magnetically characterized mixed bridged complexes, only three are reported in which the carboxylato and azido group form a mixed double bridge,[40] and in other seven they form mixed triple bridges between the Ni(II) ions. The structures of these triple bridged compounds show one example each of a two-dimensional polymer[41] with alternating double EO azido bridges and (EO-azide)bis(carboxylate) bridges, a hexanuclear complex with azido, acetato, and

dx.doi.org/10.1021/ic300547w | *Inorg. Chem.* 2012, 51, 8150−8160

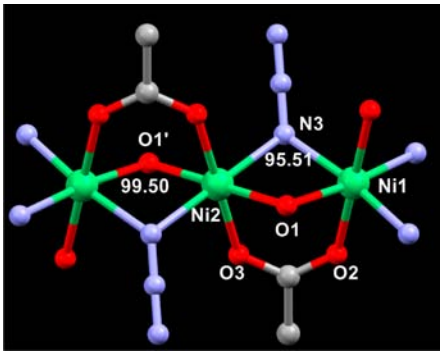

Figure 10. The coordination environment of the Ni(II) ions in compound **1** showing the bridging angles (in deg).

carbonato bridges,[42] a Ni_9 cluster containing *syn-syn* carboxylate, EO azido, and an oxido from a di-2-pyridyl ketone ligand,[43a] a Ni_5 cluster having two different set of triple bridges: one EO azido, *syn-syn* μ_2:η^1:η^1 and *syn-syn-anti* μ_3:η^1:η^2 acetate and another EO azido, *syn-syn* μ_2:η^1:η^1 acetate and methoxido[43b] and a Ni_6 cluster in which two nickel atoms are bridged through EO azido, carbonato and methoxy oxygen atom of the organic ligand.[43c] An octa-nuclear Ni(II) polyoxometalate cluster has been also reported with acetate, azido(disordered), and oxido bridges.[43d] A similar trinuclear core like compound **1** has been reported earlier (but without the magnetic study) in which two adjacent nickel atoms are linked through an EO azido, $\mu_{1,3}$-acetate and one phenoxido oxygen atom of the tridentate Schiff base ligand.[43e] Therefore, complex **1** is only the second example of a triple bridged trinuclear complex involving azido, phenoxido, and acetato ligands between Ni(II) ions. In complex **1**, Ni−N−Ni angle is 95.51(12)° indicating a ferromagnetic coupling through this pathway whereas the antiferromagnetic exchange is expected through the *syn-syn* carboxylate bridge both of which have been confirmed by DFT calculations. On the other hand, though the Ni−O−Ni angle of 99.50(13)° is ordinarily expected to transmit antiferromagnetic coupling, our DFT calculations show that it is in fact a ferromagnetic coupler in compound **1**.

Complex **2** is an EE azido bridged 1D polynuclear chain in which the basic building block is di-μ_2-phenoxido and EO azido bridged dinuclear entity. Usually the di-μ_2-pheoxido dinuclear complexes are found to be antiferromagnetic. However, we found earlier that[14b,17] if an additional single atom bridge (e.g., aqua) is introduced in such dinuclear units that may bring down the Ni−O(phenoxido)−Ni angle to a value lower than the critical one, and consequently make the exchange coupling ferromagnetic. In the present compound, the Ni−O(phenoxido)−Ni bridging angle is 85.87(6)°, which is in the range of ferromagnetic interactions. Therefore, in the dinuclear core both EO azido and phenoxido bridges transmit ferromagnetic interaction as was confirmed by DFT calculations. There are many single EE azido bridged Ni(II) 1D polynuclear complexes,[7,44] and this bridge is well-known for transmitting antiferromagnetic coupling. For this bridge, the Ni−N−N angle and the Ni−N_{azide}−Ni torsion angle are the most significant structural parameters that influence the magnitude of coupling. The maximum antiferromagnetic coupling is expected for Ni−N−N angles close to 108°, and this coupling decreases at higher values with an accidental orthogonality valley centered at 165°. On the other hand, the highest antiferromagnetic coupling appears when the torsion angle is 0° (or 180°) and diminishes when the torsion angle increases.[45] In compound **2** the Ni−N−N angle is 118.60(16)° and the Ni−N_{azide}−Ni torsion angle is 42.68(8)°, both of which indicate a weak antiferromagnetic coupling as is confirmed by DFT study (Table 4).

It is worth to mention here that quite a few dinuclear Ni(II) complexes of mixed μ_2-phenoxido and EO azido bridges are reported in the literature.[46] However, the triply bridged (di-μ_2-phenoxido and EO azido) dinuclear core as in compound **2** is a new entity (Figure 11). Thus the 1D topology of compound **2**

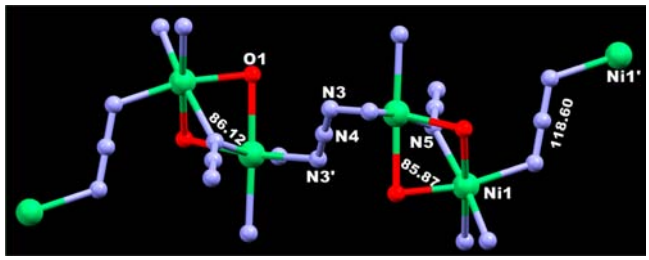

Figure 11. The coordination environment of the Ni(II) ions in compound **2** showing the bridging angles (in deg).

in which a ferromagnetic dinuclear nickel(II) core is joined by EE azido bridges is unprecedented although the alternating EO and EE azido bridged chain of Ni(II) are well documented.[10a,47]

CONCLUSION

Two complexes have been synthesized using a tridentate N,N,O donor Schiff base ligand (2-[(3-dimethylaminopropylimino)-methyl]-phenol) along with N_3^- and CH_3COO^- (for **1**) and only N_3^- (for **2**) as anionic coligands. Compound **1** presents a rare mixed tribridged (phenoxido, $\mu_{1,1}$-azido and *syn-syn* carboxylato) linear trinuclear Ni(II) complex whereas compound **2** is an unprecedented 1D polymer in which the basic Ni_2 units, formed by a new combination of mixed bridges (double phenoxido and $\mu_{1,1}$-azido), are joined through a single $\mu_{1,3}$-azido bridge. Compound **1** shows a dominant ferromag-

Table 4. Comparison of Magneto-Structural Parameters and DFT Results of Compounds 1, 2

complex	experimental J value in cm^{-1}	phenoxido bridged Ni−O−Ni angles and distances	EO azido bridged Ni−N−Ni angles and distances	Ni···Ni distances	theoretical J values in cm^{-1}
$[Ni_3L_2(OAc)_2(N_3)_2(H_2O)_2]\cdot 2H_2O$ (**1**)	16.51(6)	99.50(13)°	95.51(12)°		+32
		2.023(3) Å	2.112(3)Å	3.110(2) Å	
		2.051(3) Å	2.089(3)Å		
$[Ni_2(\mu_{1,1}\text{-}N_3)(\mu_{1,3}\text{-}N_3)(L)_2]_n$ (**2**)	J_F = +34.2(2.8)	85.86(6)°	86.12(10)°	2.857(2) Å	J_F = +59
	J_{AF} = −21.6(1.1)	2.008(2) Å	2.092(2) Å		J_{AF} = −32
		2.182(2) Å			

dx.doi.org/10.1021/ic300547w | Inorg. Chem. 2012, 51, 8150−8160

netic behavior which is a result of ferromagnetic interactions via both EO azido and phenoxido bridges and antiferromagnetic interaction through a *syn-syn* carboxylate bridge as is confirmed by DFT calculations. In complex **2**, the three single-atom bridges between Ni(II) atoms make the phenoxido bridging angle small (85.86(6)°) and consequently it transmits ferromagnetic interaction along with the EO azido-bridge within the dinuclear units, and antiferromagnetic coupling is exhibited through the single EE azido-bridge. The DFT calculations have been done to understand the overall magnetic behavior of the compounds and also to find the contribution of each bridge. Theoretical results afford a satisfactory agreement with the experimental observations.

■ ASSOCIATED CONTENT

Supporting Information

Crystallographic data in CIF format. Further details are given in Tables S1 and S2. This material is available free of charge via the Internet at http://pubs.acs.org.

■ AUTHOR INFORMATION

Corresponding Author

*E-mail: ghosh_59@yahoo.com.

Notes

The authors declare no competing financial interest.

■ ACKNOWLEDGMENTS

We thank CSIR, Government of India [Senior Research Fellowship to R.B, S.M., and P.K., Sanction nos. 09/028(0746)/2009-EMR-I, 09/079(2151)/2007-EMR-I, and 09/028(0733)/2008-EMR-I]. Crystallography was performed at the DST-FIST, India-funded Single Crystal Diffractometer Facility at the Department of Chemistry, University of Calcutta. We are thankful to Dr. You song, Nanjing University, China, and Dr. P. S. Mukherjee, IISc, India, for the magnetic data and discussion on magnetic results.

■ REFERENCES

(1) (a) Farnum, G. A.; Nettleman, J. H.; LaDuca, R. L. *CrystEngComm* **2010**, *12*, 888−897. (b) Janiak, C. *Dalton Trans.* **2003**, 2781−2804.

(2) (a) Kitagawa, S.; Kitaura, R.; Noro, S.-I. *Angew. Chem., Int. Ed.* **2004**, *43*, 2334−2375. (b) Stamatatos, T. C.; Efthymiou, C. G.; Stoumpos, C. C.; Perlepes, S. P. *Eur. J. Inorg. Chem.* **2009**, 3361−3391.

(3) Zeng, M.-H.; Zhang, W.-X.; Sun, X.-Z.; Chen, X.-M. *Angew. Chem., Int. Ed.* **2005**, *44*, 3079−3082.

(4) Wang, X.-Y.; Wang, L.; Su, G.; Gao, S. *Chem. Mater.* **2005**, *17*, 6369−6380.

(5) Mukherjee, P.; Drew, M. G. B.; Gomez-García, C. J.; Ghosh, A. *Inorg. Chem.* **2009**, *48*, 4817−4827.

(6) (a) Bonnet, M. L.; Aronica, C.; Chastanet, G.; Pilet, G.; Luneau, D.; Mathoniere, C.; Clerac, R.; Robert, V. *Inorg. Chem.* **2008**, *47*, 1127−1133. (b) Escuer, A.; Mautner, F. A.; Goher, M. A. S.; Abu-Youssef, M. A. M.; Vicente, R. *Chem. Commun.* **2005**, 605−607. (c) Ribas, J.; Monfort, M.; Diaz, C.; Bastos, C.; Solans, X. *Inorg. Chem.* **1994**, *33*, 484−489. (d) Escuer, A.; Vicente, R.; Fallah, M. S. E.; Solans, X.; Font-Bardia, M. *Inorg. Chim. Acta* **1996**, *247*, 85−91. (e) Chaudhuri, P.; Wagner, R.; Khanra, S.; Weyhermüller, T. *Dalton Trans.* **2006**, 4962−4968.

(7) (a) Massoud, S. S.; Mautner, F. A.; Vicente, R.; Gallo, A. A.; Ducasse, E. *Eur. J. Inorg. Chem.* **2007**, 1091−1102. (b) Goher, M. A. S.; Escuer, A.; Mautner, F. A.; Al-Salem, N. A. *Polyhedron* **2002**, *21*, 1871−1876.

(8) (a) Cortes, R.; Pizarro, J. L.; Lezama, L.; Arriortua, M. I.; Rojo, T. *Inorg. Chem.* **1994**, *33*, 2697−2700. (b) Karmakar, T. K.; Chandra, S. K.; Ribas, J.; Mostafa, G.; Luc, T. H.; Ghosh, B. K. *Chem. Commun.* **2002**, 2364−2365. (c) Sarkar, S.; Mondal, A.; Fallah, M. S. E.; Ribas, J.; Chopra, D.; Stoeckli-Evans, H.; Rajak, K. K. *Polyhedron* **2006**, *25*, 25−30.

(9) Hong, C. S.; Do, Y. *Angew. Chem., Int. Ed.* **1999**, *38*, 193−195.

(10) (a) Ribas, J.; Monfort, M.; Ghosh, B. K.; Solans, X. *Angew.Chem., Int. Ed. Engl.* **1994**, *33*, 2087−2089. (b) Monfort, M.; Resino, I.; Ribas, J.; Solans, X.; Font-Bardia, M.; Rabu, P.; Drillon, M. *Inorg. Chem.* **2000**, *39*, 2572−2576. (c) Abu-Youssef, M. A. M.; Escuer, A.; Goher, M. A. S.; Mautner, F. A.; Reiss, G. J.; Vicente, R. *Angew. Chem., Int. Ed.* **2000**, *39*, 1624−1626. (d) Liu, F.-C.; Zeng, Y.-F.; Zhao, J.-P.; Hu, B.-W.; Bu, X.-H.; Ribas, J.; Cano, J. *Inorg. Chem.* **2007**, *46*, 1520−1522. (e) Gao, E.-Q.; Bai, S.-Q.; Yue, Y.-F.; Wang, Z.-M.; Yan, C.-H. *Inorg. Chem.* **2003**, *42*, 3642−3649.

(11) (a) Thompson, L . K.; Xu, Z. Q.; Goeta, A. E.; Howard, J. A. K.; Clase, H. J.; Miller, D. O. *Inorg. Chem.* **1998**, *37*, 3217−3229. (b) Graham, B.; Hearn, M. T. W.; Junk, P. C.; Kepert, C. M.; Mabbs, F. E.; Moubaraki, B.; Murray, K. S.; Spiccia, L. *Inorg. Chem.* **2001**, *40*, 1536−1543 and references therein.

(12) Agnus, Y.; Lewis, R.; Gisselbrecht, J. P.; Weiss, R. *J. Am. Chem. Soc.* **1984**, *106*, 93−102.

(13) (a) Nishida, Y.; Takeuchi, M.; Takahashi, K.; Kida, S. *Chem. Lett.* **1985**, 631−634. (b) Nishida, Y.; Takeuchi, M.; Takahashi, K.; Kida, S. *Chem. Lett.* **1983**, 1815−1818. (c) McKee, V.; Zvagulis, M.; Reed, C. A. *Inorg. Chem.* **1985**, *24*, 2914−2919.

(14) (a) Nanda, K. K.; Das, R.; Thompson, L. K.; Venkatsubramanian, K.; Nag, K. *Inorg. Chem.* **1994**, *33*, 5934−5939. (b) Biswas, R.; Giri, S.; Saha, S. K.; Ghosh, A. *Eur. J. Inorg. Chem.* **2012**, 2916−2927.

(15) (a) Ray, M. S.; Ghosh, A.; Das, A.; Drew, M. G. B.; Ribas-Ariño, J.; Novoa, J.; Ribas, J. *Chem. Commun.* **2004**, 1102−1103. (b) Wang, Z.; Zhang, B.; Kurmoo, M.; Green, M. A.; Fujiwara, H.; Otsuka, T.; Kobayashi, H. *Inorg. Chem.* **2005**, *44*, 1230−1237. (c) Wang, Z.; Zhang, B.; Inoue, K.; Fujiwara, H.; Otsuka, T.; Kobayashi, H.; Kurmoo, M. *Inorg. Chem.* **2007**, *46*, 437−445. (d) Liu, T.; Zhang, Y.; Yang, Z.; Gao, S. *Inorg. Chem.* **2006**, *45*, 2782−2784.

(16) (a) Sengupta, O.; Gole, B.; Mukherjee, P. S. *Inorg. Chim. Acta* **2010**, *36*, 33093−3101. (b) Sengupta, O.; Gole, B.; Mukherjee, P. S. *Polyhedron* **2010**, *29*, 2945−2952.

(17) Biswas, R.; Kar, P.; Song, Y.; Ghosh, A. *Dalton Trans.* **2011**, *40*, 5324−5331.

(18) (a) Dutta, R. L.; Syamal, A. *Elements of Magnetochemistry*, 2nd ed.; East West Press: Manhattan Beach, CA, 1993. (b) Kahn, O. *Molecular Magnetism*; VCH publisher: New York, 1993.

(19) Sheldrick, G. M. *SHELXS 97, Program for Structure Solution*; University of Göttingen: Göttingen, Germany, 1997.

(20) Sheldrick, G. M. *SHELXL 97, Program for Crystal Structure Refinement*; University of Göttingen: Göttingen, Germany, 1997.

(21) Spek, A. L. *J. Appl. Crystallogr.* **2003**, *36*, 7−13.

(22) Farrugia, L. J. *J. Appl. Crystallogr.* **1997**, *30*, 565−566.

(23) Farrugia, L. J. *J. Appl. Crystallogr.* **1999**, *32*, 837−838.

(24) Ruiz, E.; Alemany, P.; Alvarez, S.; Cano, J. *J. Am. Chem. Soc.* **1997**, *119*, 1297−1303.

(25) Ruiz, E.; Rodríguez-Fortea, A.; Cano, J.; Alvarez, S.; Alemany, P. *J. Comput. Chem.* **2003**, *24*, 982−989.

(26) Ruiz, E.; Cano, J.; Alvarez, S.; Alemany, P. *J. Comput. Chem.* **1999**, *20*, 1391−1400.

(27) Ruiz, E. *Struct. Bonding (Berlin)* **2004**, *113*, 71−83.

(28) (a) Sarkar, S.; Datta, A.; Mondal, A.; Chopra, D.; Ribas, J.; Rajak, K. K.; Sairam, S. M.; Pati, S. K. *J. Phys. Chem. B* **2006**, *110*, 12−15. (b) Mukherjee, S.; Gole, B.; Chakrabarty, R.; Mukherjee, P. S. *Inorg. Chem.* **2009**, *48*, 11325−11334. (c) Mukherjee, S.; Gole, B.; Song, Y.; Mukherjee, P. S. *Inorg. Chem.* **2011**, *50*, 3621−3631. (d) Sengupta, O.; Gole, B.; Mukherjee, S.; Mukherjee, P. S. *Dalton Trans.* **2010**, *39*, 7451−7465. (e) Mukherjee, S.; Patil, Y. P.; Mukherjee, P. S. *Dalton Trans.* **2012**, *41*, 54−64. (f) Mukherjee, S.; Patil, Y. P.; Mukherjee, P. S. *Inorg. Chem.* **2012**, *51*, 4888−4890.

(29) Becke, A. D. *J. Chem. Phys.* **1993**, *98*, 5648−5652.

(30) Frisch, M. J.; Trucks, G. W.; Schlegel, H. B.; Scuseria, G. E.; Robb, M. A.; Cheeseman, J. R.; Montgomery, J. A.; Vreven, T.; Kudin, K. N.; Burant, J. C.; Millam, J. M.; Iyengar,S. S.; Tomasi, J.; Barone, V.; Mennucci, B.; Cossi, M.; Scalmani, G.; Rega, N.; Petersson, G. A.; Nakatsuji, H.; Hada, M.; Ehara, M.; Toyota, K.; Fukuda, R.; Hasegawa, J.; Ishida, H.; Nakajima, T.; Honda, Y.; Kitao, O.; Nakai, H.; Klene, M.; Li, X.; Knox, J. E.; Hratchian, H. P.; Cross, J. B.; Adamo, C.; Jaramillo, J.; Gomperts, R.; Stratmann, R. E.; Yazyev, O.; Austin, A. J.; Cammi, R.; Pomelli, C.; Ochterski, J.; Ayala, P. Y.; Morokuma, K.; Voth, G. A.; Salvador, P.; Dannenberg, J. J.; Zakrzewski, V. G.; Dapprich, S.; Daniels, A. D.; Strain, M. C.; Farkas, O.; Malick, D. K.; Rabuck, A. D.; Raghavachari, K.; Foresman, J. B.; Ortiz, J. V.; Cui, Q.; Baboul, A. G.; Clifford, S.; Cioslowski, J.; Stefanov, B. B.; Liu, G.; Liashenko, A.; Piskorz, P.; Komaromi, I.; Martin, R. L.; Fox, D. J.; Keith, T.; Al-Laham, M. A.; Peng, C. Y.; Nanayakkara, A.; Challacombe, Gill, M.; P. M.; Johnson, W. B.; Chen, W.; Wong, M. W.; Gonzalez, C.; Pople, J. A. *Gaussian 03*, revision B.4; Gaussian Inc.: Pittsburgh, PA, 2003.
(31) Becke, A. D. *Phys. Rev. A* **1988**, *38*, 3098−3100.
(32) Lee, C.; Yang, W.; Parr, R. G. *Phys. Rev. B* **1988**, *37*, 785−789.
(33) Ruiz, E.; Alvarez, S.; Cano, J.; Polo, V. *J. Chem. Phys.* **2005**, *123*, 164110−164117.
(34) Schäfer, A.; Huber, C.; Ahlrichs, R. *J. Chem. Phys.* **1994**, *100*, 5829−5835.
(35) Bacskay, G. B. *Chem. Phys.* **1981**, *61*, 385−404.
(36) Gomes, L.; Pereira, E.; De, B. C. *J. Chem. Soc., Dalton Trans.* **2000**, 1373−1379.
(37) Escuer, A.; Vicente, R.; Fallah, M. S. E.; Kumar, S. B.; Mautner, F. A.; Gatteschi, D. *Dalton Trans.* **1998**, 3905−3909.
(38) (a) Haldane, F. D. M. *Phys. Rev. Lett.* **1983**, *50*, 1153−1156. (b) Haldane, F. D. M. *Phys. Lett. A* **1983**, *93*, 464−468. (c) Renard, J. P.; Verdaguer, M.; Regnault, L. P.; Erkelens, W. A. C.; Rossat-Mignon, J.; Stirling, W. G. *Europhys. Lett.* **1987**, *3*, 945−951. (d) Renard, J. P.; Verdaguer, M.; Regnault, L. P.; Erkelens, W. A. C.; Rossat-Mignon, J.; Ribas, J.; Stirling, W. J.; Vettier, C. *J. Appl. Phys.* **1988**, *63*, 3538−3543.
(39) (a) Nanda, K. K.; Das, R.; Thompson, L. K.; Venkatsubramanian, K.; Paul, P.; Nag, K. *Inorg. Chem.* **1994**, *33*, 1188−1193. (b) Mukherjee, P.; Drew, M. G. B.; Gomez-García, C. J.; Ghosh, A. *Inorg. Chem.* **2009**, *48*, 5848−5860.
(40) (a) Milios, C. J.; Prescimone, A.; Sanchez-Benitez, J.; Parsons, S.; Murrie, M.; Brechin, E. K. *Inorg. Chem* . **2006**, *45*, 7053−7055. (b) Meyer, F.; Demeshko, S.; Leibeling, G.; Kersting, B.; Kaifer, E.; Pritzkow, H. *Chem.—Eur. J.* **2005**, *11*, 1518−1526. (c) Meyer, F.; Kircher, P.; Pritzkow, H. *Chem. Commun.* **2003**, 774−775.
(41) Sun, W.-W.; Tian, C.-Y.; Jing, X.-H.; Wang, Y.-Q.; Gao, E.-Q. *Chem. Commun.* **2009**, 4741−4743.
(42) Tong, M.-L.; Monfort, M.; Juan, J. M. C.; Chen, X.-M.; Bu, X.-H.; Ohba, M.; Kitagawa, S. *Chem.Commun.* **2005**, 233−235.
(43) (a) Papaefstathiou, G. S.; Boudalis, A. K.; Stamatatos, T. C.; Milios, C. J.; C. Efthymiou, G.; Raptopoulou, C. P.; Terzis, A.; Psycharis, V.; Sanakis, Y.; Vicente, R.; Escuer, A.; Tuchagues, J.-P.; Perlepes, S. P. *Polyhedron* **2007**, *26*, 2089−2094. (b) Boudalis, A. K.; Pissas, M.; Raptopoulou, C. P.; Psycharis, V.; Abarca, B.; Ballesteros, R. *Inorg. Chem.* **2008**, *47*, 10674−10681. (c) Georgopoulou, A. N.; Raptopoulou, C. P.; Psycharis, V.; Ballesteros, R.; Abarca, B.; Boudalis, A. K. *Inorg. Chem.* **2009**, *48*, 3167−3176. (d) Pichon, C.; Mialane, P.; Dolbecq, A.; Marrot, J.; Rivière, E.; Bassil, B. S.; Kortz, U.; Keita, B.; Nadjo, L.; Sécheresse, F. *Inorg. Chem.* **2008**, *47*, 11120−11128. (e) Cao, G.-B. *Synth. React. Inorg. Met-Org. Nano-Met. Chem.* **2007**, *37*, 639−642.
(44) (a) Manna, S. C.; Konar, S.; Zangrando, E.; Drew, M. G. B.; Ribas, J.; Chaudhuri, N. R. *Eur. J. Inorg. Chem.* **2005**, 1751−1758. (b) Monfort, M.; Resino, I.; Fallah, M. S. E.; Ribas, J.; Solans, X.; Font-Bardia, M.; Stoeckli-Evans, H. *Chem.—Eur. J.* **2001**, *7*, 280−287.
(45) Monfort, M.; Resino, I.; Ribas, J.; Solans, X.; Font-Bardia, M.; Stoeckli-Evans, H. *New J. Chem.* **2002**, *26*, 1601−1606.
(46) (a) Dey, S. K.; Mondal, N.; Fallah, M. S. E.; Vicente, R.; Escuer, A.; Solans, X.; Font-Bardía, M.; Matsushita, T.; Gramlich, V.; Mitra, S. *Inorg. Chem.* **2004**, *43*, 2427−2434. (b) Banerjee, A.; Singh, R.; Chopra, D.; Colacio, E.; Rajak, K. K. *Dalton Trans.* **2008**, 6539−6545. (c) Zhang, Y.; Zhang, X.-M.; Liu, T.-F.; Xu, W.-G. *Transition Met.Chem.* **2010**, *35*, 851−858. (d) Sasmal, S.; Hazra, S.; Kundu, P.; Dutta, S.; Rajaraman, G.; Sanudo, E. C.; Mohanta, S. *Inorg. Chem.* **2011**, *50*, 7257−7267.
(47) Ribas, J.; Monfort, M.; Resino, I.; Solans, X.; Rabu, P.; Maingot, F.; Drillon, M. *Angew. Chem., Int. Ed. Engl.* **1996**, *35*, 2520−2522.